Experimental Study of the Development of Longitudinal Vortex Pairs Embedded in a Turbulent Boundary Layer

Wayne R. Pauley* and John K. Eaton†
Stanford University, Stanford, California

The mean streamwise development of pairs of longitudinal vortices and arrays of longitudinal vortices embedded in an otherwise two-dimensional turbulent boundary layer is studied. Planes of closely spaced measurements of the three components of mean velocity were obtained at several streamwise locations, and the vorticity and circulation were calculated. It was found that the rate of vorticity spreading in a vortex was greatly increased by close proximity of other vortices. Vortices remaining close to the wall produced significant levels of spanwise skin friction and, thus, a greater rate of streamwise circulation decrease.

Nomenclature

Cf = skin friction coefficient
U = mean velocity in X direction
Ue = velocity at edge of boundary layer
V = mean velocity in Y direction
W = mean velocity in Z direction
X = streamwise coordinate (measured from test section inlet)
Y = vertical coordinate (measured from test wall)
Z = spanwise coordinate (measured from tunnel centerline)
δ_{99} = $u/ue = 0.99$
Γ_{POS} = positive circulation (only positive regions included)
Ω = streamwise vorticity
Ω_{max} = maximum streamwise vorticity

I. Introduction

LONGITUDINAL vortices embedded in turbulent boundary layers occur naturally in many flows and are purposely induced in other flows. Naturally occurring vortices are often found in pairs, such as the horseshoe vortex pair produced by a blunt protuberance from a surface. Arrays of vortices are often introduced to prevent boundary-layer separation on lifting and control surfaces. With the present emphasis on high performance near stall there is considerable interest in better understanding and prediction of the streamwise development of longitudinal vortices embedded in turbulent boundary layers.

There have been several previous studies of embedded vortices that are relevant to the present work. Pearcy[1] presented a review of measurements for a wide range of vortex arrays. Using measurement of the mean axial velocity made by several researchers, he tracked the locations of the vortices and determined the extent of boundary-layer modification due to their presence. He developed rules for the design of vortex generator arrays to forestall boundary-layer separation, but left considerable doubt about how the interaction between the vortices modified their streamwise persistence. His conclusions suggest that further study of the interaction between embedded longitudinal vortices is necessary to understand and predict their behavior. Spangler and Wells[2] reviewed the work of previous groups studying the effects of vortices on drag, and did a detailed study of the local skin friction modification due to the presence of vortices. They concluded that the vortices substantially increase the skin friction in downwash regions where the boundary layer is thinned.

Mehta et al.[3] provided a detailed set of data at one streamwise location for each of two embedded vortex pair cases, one in which the common flow between the pair was directed away from the wall, and one in which the flow between the pair was directed toward the wall. The focus of the work was on the turbulence structure in the disturbed boundary layer. None of the previous studies have focused on the streamwise development of embedded vortices while interacting with other vortices. Westphal et al.[4] examined the development of single vortices in both zero and adverse pressure gradients. The present work extends that work to a variety of multiple vortex situations.

The interaction between adjacent vortices can be divided into two types, counter-rotating and corotating, based on their relative sense of rotation. Counter-rotating vortices are identified by the direction of the secondary flow between them that can be directed either toward or away from the wall. Following Mehta et al.[3] we denote these cases "common flow down" and "common flow up," respectively. To discuss the development and mean motion of vortices it is necessary to have a consistent definition of the strength and location of a single vortex. Work by Westphal et al.[4,5] has shown that circulation and the point of maximum vorticity in the vortex are good descriptors of the vortex strength and location, respectively. These quantities can be accurately calculated using closely spaced measurements of the three components of the mean velocity.

In the present study, we have made extensive three-component mean velocity measurements for 16 different vortex pair configurations and two regular arrays (see Table 1). The vortices were embedded in a zero pressure gradient turbulent boundary layer for all of the cases examined. The data increase our understanding of the development of embedded streamwise vortices while interacting with other streamwise vortices.

II. Experimental Techniques

The experiment was carried out in the blower-driven, two-dimensional, boundary-layer wind tunnel shown in Fig. 1. Not shown in the figure are the upstream flow conditioning elements that provide uniform two-dimensional flow at the test section inlet with a freestream turbulence intensity of approximately 0.2%. The facility has a 200-cm-long test section and operates at a nominal freestream velocity of 16 m/s. One wall

Received April 16, 1987; presented as Paper 87-1309 at the AIAA 19th Fluid Dynamics, Plasma Dynamics and Laser Conference, Honolulu, HI, June 8–10, 1987; revision received Sept. 14, 1987. Copyright © American Institute of Aeronautics and Astronautics, Inc., 1988. All rights reserved.

*Research Assistant, Department of Mechanical Engineering; currently Assistant Professor, Department of Aerospace Engineering, The Pennsylvania State University. Member AIAA.

†Associate Professor, Department of Mechanical Engineering. Member AIAA.

of the test section is used as the test wall on which the boundary layer forms, the other contains slotted ports for instrumentation access. Further details about the facility are given by Eibeck and Eaton.[6] Half-delta-wing generators 2 cm high and 5 cm long were mounted at angle of attack on the test wall 53 cm downstream of the boundary-layer trip. At that location the undisturbed boundary-layer thickness was 1.3 cm and the momentum thickness Reynolds number was 1700. The spacing between the generators was measured at their midlength and their angles of attack were measured between the vortex generators and the test wall centerline.

Measurements were made using a miniature five-hole pressure probe positioned using a two-axis computer-controlled traverse. The five-hole probe tip was 2.7 mm in diameter with 0.4 mm pressure ports on 45-deg facets. The probe was calibrated using a simplification of the method described by Treaster and Yocum.[7] These measurements were corrected for the effects of lateral gradients in streamwise velocity using a first-order scheme; the local gradients in the mean velocity were computed, and the secondary velocities due to them were removed. Without this correction, the pressure differences across the finite width of the probe caused by lateral gradients of the streamwise velocity would be incorrectly interpreted as secondary velocities. The calibration and gradient correction are described in detail by Westphal et al.[5] The uncertainty of the mean flow measurements is ± 0.5 deg for the flow angles and $\pm 5\%$ for the magnitude of the velocity vector. Data acquisition and probe placement were controlled by a DEC MINC laboratory computer. Data processing was done off-line on a VAX 11/750 computer. Skin friction was measured using the dual sublayer fence probe described by Higuchi.[8] This probe allowed resolution of both streamwise and spanwise components of the skin friction.

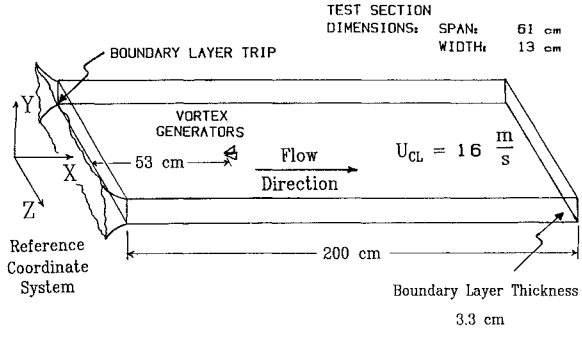

Fig. 1 Boundary-layer wind-tunnel test section.

III. Results and Discussion

Figure 2 shows a typical plane of mean velocity data for one-half of a vortex pair that is centered at $Z=0.0$. The secondary flow velocity vectors shown in a Y-Z plane looking downstream (Fig. 2a) exhibit characteristics very similar to Rankine vortices with images to account for the effects of the solid wall. All of the vortices studied were fairly weak, with the maximum secondary flow angle less than 25 deg. The axial velocity contours (Fig. 2b) illustrate the strong distortion of the boundary layer by the vortices. The outer contour indicates the location of the edge of the boundary layer (δ_{99}). The inter-

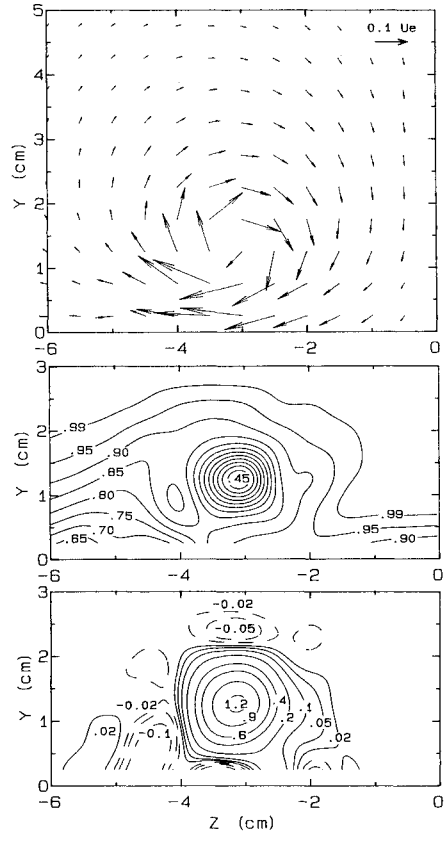

Fig. 2 Secondary velocity vectors, streamwise velocity contours, and streamwise vorticity contours. (Detailed view of $X=66$-cm station for case shown in Figs. 4a–4c.)

Table 1 Vortex pair study mean flow and skin friction measurements

Case number	Number of data planes	Description	Generator height, cm	Spacing, cm	Angle of attack, deg	X locations mean data, cm	Skin friction at $X=97$ cm
1	4	Common down	2	2	18	66,97,142,188	Center
2	4	Common down	2	3	18	66,97,142,188	Center
3	4	Common down	2	4	18	66,97,142,188	Span
4	2	Common down	2	6	18	66,97	Center
5	3	Common down	2	10	18	66,97,188	Center
6	1	Common down	2	14	18	97	Center
7	1	Common down	2	4	6	97	Center
8	1	Common down	2	4	12	97	Center
9	1	Common down	2	4	24	97	Center
10	4	Commom up	2	4	18	66,97,142,188	Span
11	1	Commom up	2	10	18	188	None
12	1	Commom up	2	14	18	188	None
13	4	Unequal	2/1	4	18/18	66,97,142,188	None
14	4	Co-Rotating	2	4	18	66,97,142,188	None
15	1	Co-Rotating	2	6	18	188	None
16	1	Co-Rotating	2	10	18	188	None
17	4	Co-Rotating array	2	6	18	66,97,142,188	None
18	4	Alternating array	2	10	18	66,97,142,188	None

val between successive contours is 5% of the freestream velocity. This convention will be used throughout for the contours of axial velocity.

The main focus of this paper is on the downstream development of the embedded vortices, which is best studied by examination of the vorticity contour plots. The contour levels shown in Fig. 2c will be used for all subsequent vorticity plots to facilitate comparison of vortex size and intensity between cases. Dotted lines on these contour plots indicate regions of negative vorticity. This vorticity distribution is typical of that seen at the upstream station nearest to the vortex generator where the vortices are the strongest. The vorticity contours within the vortex out to the 0.2-cm contour are quite circular. The interaction of the secondary flow and the no-slip condition at the wall produces the region of negative vorticity below the vortex. This negative vorticity is convected by the primary vortex and accumulates on the up-wash side of the vortex. As the vortex develops downstream the accumulation of negative vorticity grows, but a clear rollup of a secondary vortex is never observed.

The spanwise component of the wall skin friction is the only means by which a single vortex can lose circulation. The vorticity of an embedded vortex, however, is diffused rapidly and the vortex grows. The rapid diffusion is caused by strong gradients in the normal stress anisotropy ($\overline{v'^2} - \overline{w'^2}$) and in the crossflow-plane shear stress ($\overline{v'w'}$). Gradients in these quantities appear in the mean transport equation for streamwise vorticity, and contribute to the decay of the streamwise vorticity as pointed out by Perkins.[9] These gradients are set up when the vortex distorts the mean velocity and Reynolds stress field of the turbulent boundary layer as shown in Refs. 3 and 5. In addition, the streamwise velocity contours indicate a significant streamwise velocity deficit in the central region of the vortex. The mean stretching that occurs as this velocity deficit recovers produces a slight positive contribution to the streamwise vorticity.

More complicated mechanisms for vortex distortion and decay are possible when the vortex is an element of a pair. For example, the two halves of a counter-rotating vortex pair may exchange vorticity, thereby reducing the circulation of each vortex. Also, the induced velocity field of one vortex may distort the other. In the following sections we examine the axial development of various vortex pairs and vortex arrays, paying particular attention to how the development of a vortex is influenced by adjacent vortices under a variety of conditions. In each case we examine the axial development of the peak vorticity and the circulation of the primary vortex. The peak vorticity development gives an indication of how rapidly vorticity is diffused. The decay of the vortex strength indicates the rate of loss in integrated vorticity, due to the interaction with the wall or by exchange with other vortices. The circulation of the primary vortex was used as the measure of vortex strength and was defined as the integral of all positive vorticity in the data plane. This method offers the important advantage of separating the circulation of the primary vortex from that of the induced vorticity. In all cases the induced vorticity region had a circulation of 15–25% of that found in the primary vorticity region. For planes with symmetry about $Z = 0.0$, integration included only half of the data field. The other half was used separately to obtain a second estimate of the circulation and peak vorticity for purposes of checking. These comparisons always yielded differences of less than 5%.

Common Flow Down

Vortex interaction with common flow between the vortices directed toward the wall was the most extensively studied, since it caused the strongest distortion of the boundary layer over the greatest streamwise extent. A vortex pair with common flow down moves apart as it develops, producing an ever widening region of boundary-layer thinning. Two parameters were varied independently in studying these pairs: the spacing between the vortices and the vortex strength. The parameter space is shown in Fig. 3.

Data at four axial locations for a vortex generator spacing of 4 cm (2 generator heights) are shown in Figs. 4a–4c. These document important features of the development of common-flow-down pairs. The mean motion of the vortex centers qualitatively follow a two-dimensional potential flow model that represents the real vortices as point vortices with images in the solid wall. A common-flow-down pair of vortices released at some initial time will move apart due to the image flow. Replacing time in this simple model with the axial distance divided by the freestream velocity, we see that the vortices will diverge moving downstream. This potential flow description is only qualitatively useful because opposite sign vorticity is produced at the wall due to viscous forces. A region of weak opposite sign vorticity in the upwash region of the vortex (Fig. 4c) confirms this expectation.

The development of the vortex size and shape as indicated by the distribution of streamwise vorticity is similar to that seen by Westphal et al.[4] for single vortices, indicating that the vortices never interact strongly in common-flow-down cases. The peak vorticity decreased rapidly in the streamwise direction, and the area within the vorticity contours grew. The vortex did not maintain its circular shape as it grew but rather became longer in the horizontal direction. This same behavior was observed for the single vortex by Westphal et al.[4,5] who determined that the flattening was not due to vortex meandering, but left open the question of its actual cause. The present study indicates that the asymmetric spreading of vorticity seen as flattening of the vorticity contours occurs due to the proximity of the image vortex (see further discussion below).

The strength of the vortices generated was found to be independent of delta wing spacing for separations greater than 2 generator heights (Fig. 3). Delta wings spaced 2 generator heights or more apart produced the same strength vortices. Closer spacing of the generators slightly inhibits the ability of the delta wing to generate a vortex. The rate of circulation decrease in the streamwise direction was the same for all spacings, supporting the assertion made based on the vorticity contours that these vortices are not interacting strongly.

The degree and extent of boundary-layer thinning between the vortices is important because it indicates the ability of the vortices to forestall boundary-layer separation. Work by Spangler and Wells[2] and Mehta et al.[3] has shown that this is also a region of significant skin friction enhancement. The effects of varying the vortex spacing on the degree of boundary-layer thinning between the vortices is shown in Fig. 5. As the spacing of the vortex generators was increased, the thickness of the boundary layer between the vortices increased. Boundary-layer thinning was surprisingly persistent, however, extending to the largest vortex spacing studied (7 generator heights).

The effect of angle of attack on the vortex strength is shown in Fig. 3. For angles of attack less than 18 deg, the strength of the vortex pair produced increases linearly with angle of attack. Beyond this, the rate of increase decreases as expected for a delta wing generator. The degree of boundary-layer thinning at

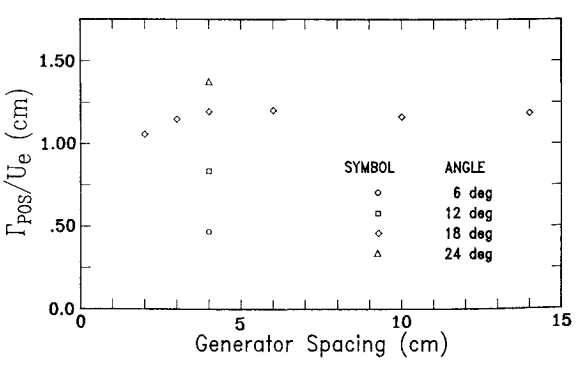

Fig. 3 Parameter space for common-flow-down study.

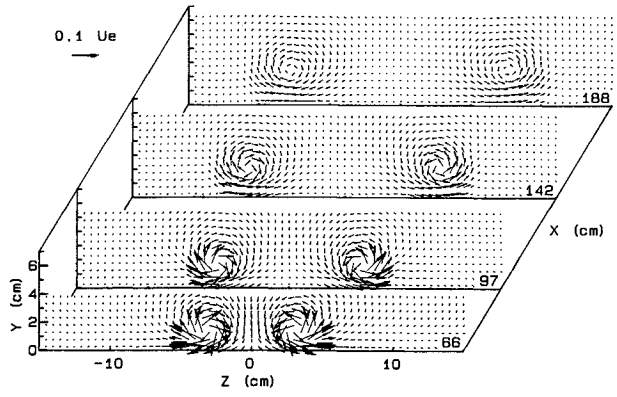

a) Secondary flow vectors

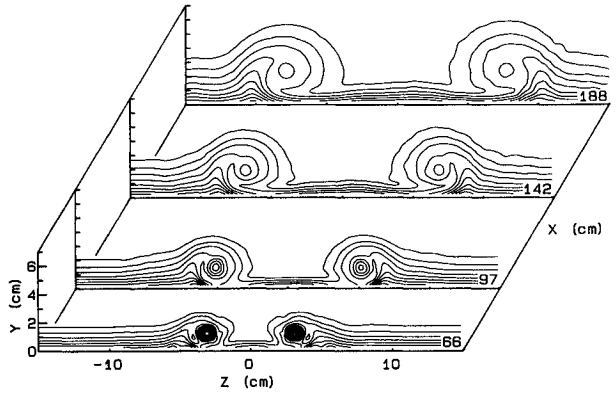

b) Contours of streamwise velocity

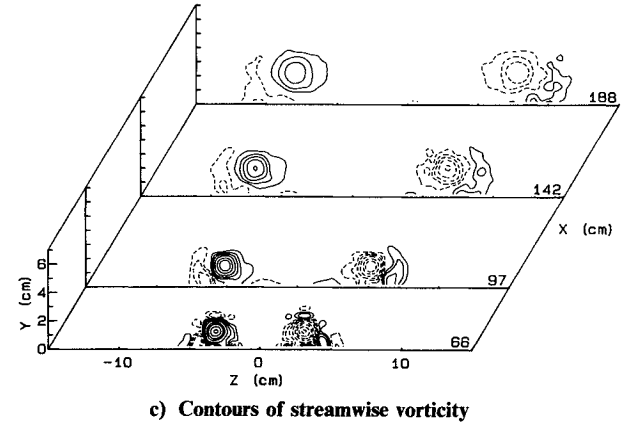

c) Contours of streamwise vorticity

Fig. 4 Study of vortex pair with common flow down (4-cm spacing, 18-deg angles).

the centerline did not vary with increasing vortex generator angle of attack. The width of the thinned region increased roughly in proportion to the vortex strength as the angle of attack was increased (see Fig. 6). The insensitivity of the boundary-layer thickness to vortex strength is apparently due to offsetting effects; the stronger image flow of the stronger vortices carries them further apart and, as a result, the secondary velocities directed toward the wall and the corresponding lateral divergence in the centerplane region are approximately the same for all cases. This results in a boundary layer between the vortices with the same boundary-layer thickness but with increased width.

Common Flow Up

Three different cases of equal strength counter-rotating vortices with the common flow up were investigated. The only

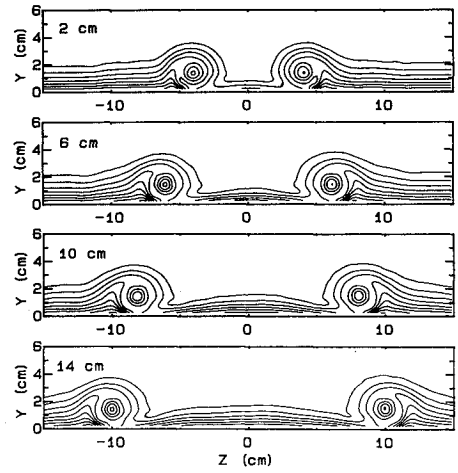

Fig. 5 Streamwise velocity contours for different spacings of delta wing vortex generators (common flow down).

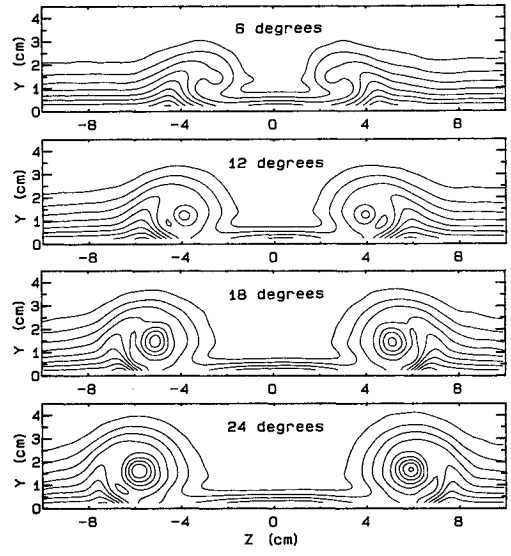

Fig. 6 Streamwise velocity contours for different delta wing vortex generator angles of attack (fixed spacing of 4 cm, common-flow-down pairs at $X=97$ cm).

parameter varied was the initial vortex spacing. The image flow causes the vortices to move toward the centerline until they get close enough together that the effects of the images nearly cancel each other. As they move close to each other at the centerline, they convect each other away from the wall. The common-flow-up vortices thus interact strongly with each other, but only weakly with the viscous flow near the wall and their image vortices. This is the opposite of the common-flow-down pair.

Figure 7 shows vorticity contours measured at $X=188$ cm for three different initial vortex spacings. The edge of the boundary layer (δ_{99}) is also shown as a dotted line. The vortices with the smallest initial spacing have lifted completely out of the boundary layer (and the measurement domain) by this station. The boundary-layer thickness is not significantly distorted except in the immediate vicinity of the vortices. The vorticity contours are strongly elongated in the vertical direction as suggested in Fig. 7 and seen more clearly in Fig. 8. The vortices with the intermediate initial spacing have lifted somewhat but are still low enough to cause a significant boundary-layer perturbation. The vorticity contours are elongated slightly in the vertical direction, indicating a significant interaction between the two vortices. The vortex pair with the widest initial spacing is still well embedded in the boundary layer and

causes a significant perturbation to the boundary-layer thickness. The vorticity contours appear to have remained round with no evidence of either vertical or horizontal elongation.

It is clear that the vortices with the closer initial spacing have a much stronger interaction. At large initial spacing, the secondary velocities decay before the vortices approach close enough to convect each other out of the boundary layer. The secondary velocities are also too weak to distort the vortex significantly.

The case with the strong vortex interaction (4-cm spacing) is examined more closely in Figs. 8a–8c. The secondary velocity vectors show that the pair produces a strong vertical flow between the vortices. It is clear, particularly at the 97-cm station, that the secondary flow due to one vortex is still significant in the vicinity of the other vortex. The axial velocity contours show that the vortices are rapidly lifted and cause a significant perturbation to the boundary layer over a relatively limited distance.

The vorticity contours show the strong distortion of the vortices. At the first station, the vorticity contours are nearly round. By the 97-cm station, the vortices have been elongated so that the vertical axis of a typical contour is over 1.5 times longer than the horizontal axis. The same degree of flattening was seen for a single vortex flow in the horizontal direction by Westphal et al.[4] indicating that the image vortex is responsible for single vortex flattening. However, the flattening in the single vortex case developed over a longer streamwise distance. The more rapid flattening observed in the present case is because the two vortices of the pair are brought into closer proximity than are the vortex and its image in the single vortex case.

The decay of the peak vorticity is more rapid in the common-flow-up cases than in the common-flow-down cases. This is probably due to the vertical spreading of the vorticity by the adjacent vortex. There is also much less generation of opposite sign vorticity at the wall. This is because the vortices are lifted away from the wall and the resulting secondary velocities near the wall are weaker.

One common-flow-up pair was studied in which the vortices were of unequal strength (see Fig. 9). The weaker vortex was generated using a half-size vortex generator so that the ratio of the vortex circulations was approximately 2. The generators were separated by 4 cm, the same as the case illustrated in Fig. 8. The weaker vortex was rapidly convected and distorted by the stronger one. At the 97-cm station, the weak vortex has been lifted well away from the wall and elongated to an aspect ratio of nearly 2 to 1. The vorticity of the weak vortex is diffused very rapidly, and by the last measurement station the diffusion is so complete that the vortex can no longer be identified. The stronger vortex is slightly distorted at the 97-cm station, but there is no evidence of distortion farther downstream.

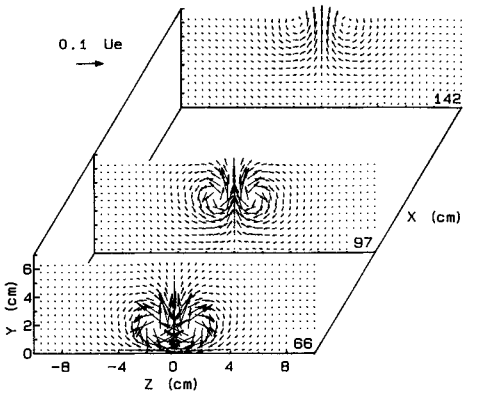

a) Secondary flow vectors

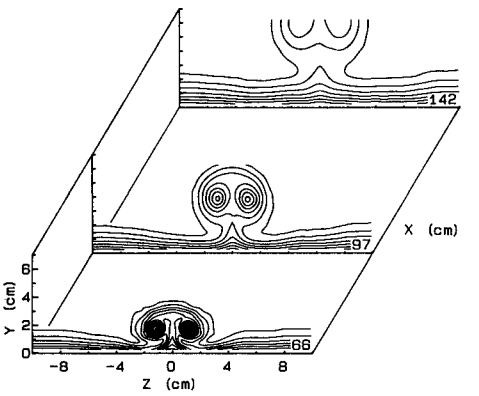

b) Streamwise velocity contours

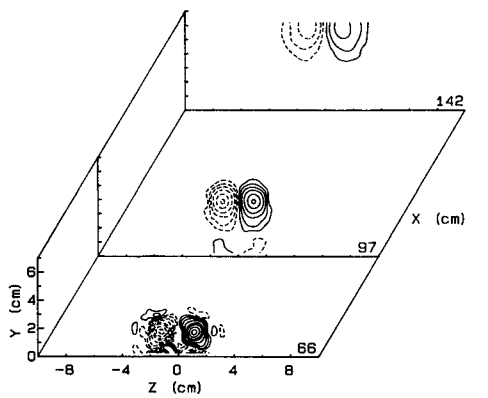

c) Streamwise vorticity contours

Fig. 8 Study of common-flow-up pairs (4-cm spacing).

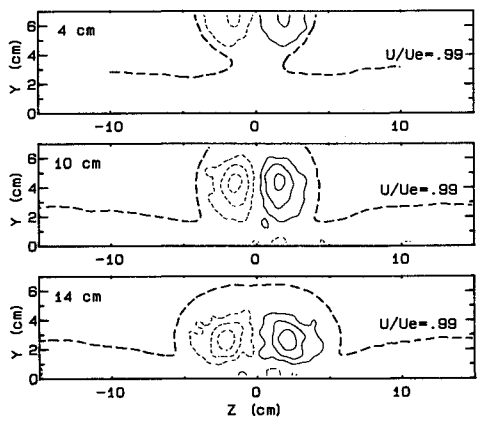

Fig. 7 Comparison of streamwise vorticity contours and 99% axial velocity contour for common-flow-up pairs with different initial spacings at $X = 188$ cm.

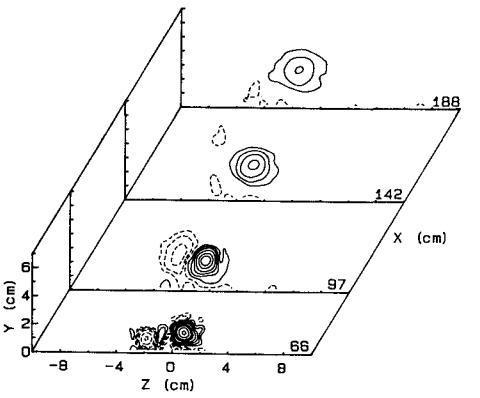

Fig. 9 Contours of streamwise vorticity for unequal-strength vortex pair with common flow up (delta wings 1- and 2-cm high, spaced 4 cm apart).

The peak vorticity in the weaker vortex decreased much more rapidly than in any other vortex studied, indicating rapid vorticity spreading. The behavior of these vortices supports the observation that strong interaction significantly increases the rate of vorticity spreading. The smaller vortex is seen to be flattened more than in any other case, supporting the observation made previously that the flattening of the vorticity contours is induced by an adjacent vortex—either a real or an image vortex.

In applications of counter-rotating vortices, the vortex generators are usually arranged to produce pairs alternating between common flow up and common flow down. To determine if regular arrays produce different vortex development than produced by pairs, a counter-rotating array was used. This array was chosen using design guidelines reported by Pearcy[2] to produce the maximum degree of boundary-layer thinning over the available length of test section. The streamwise development is shown in Fig. 10. The magnitudes of the vortex strengths and the streamwise rate of decay of the vortices observed for this array closely matched that of the common-flow-up pair with the same initial spacing. Comparing Fig. 7 and Fig. 10, we see that the positions of the vortices and shapes of the vorticity contours at $X = 188$ cm were the same as well. The common-flow-up interaction is dominant in determining the shape of the vorticity contours in this array because the image flow rapidly drives the array into a set of common-flow-up pairs. The extent of the common-flow-down region is limited in the array configuration because the vortices encounter an adjacent pair. At $X = 188$ cm, the spacing between the vortices is 17 cm instead of 22 cm, as seen for the common-flow-down pair with this initial spacing.

Co-Rotating Vortices

Many practical configurations utilize uniformly spaced arrays of co-rotating vortices. Their ability to work well in the presence of the lateral flow on swept wings makes them particularly useful in aeronautical applications. A single pair of co-rotating vortices will merge to form a single vortex if the initial spacing is not too large. Regular arrays of co-rotating vortices do not coalesce except on the ends of the array, and they do not lift out of the boundary layer. Experiments were performed on three different co-rotating pairs and one regular array of co-rotating vortices.

The measured development of a co-rotating pair with initial spacing of 4 cm is shown in Figs. 11a and 11b. This initial spacing resulted in coalescence of vortices while they remained embedded in the boundary layer. Even with this merging, vorticity was not spread as fast as observed in the common-flow-up case. This is indicated by the rate of decrease of the peak vorticity and the growth of the vorticity contours. There is an apparent shear layer in the secondary flow between the vortices that might be expected to generate increased turbulence activity and more rapid diffusion of vorticity. However, distortions in the mean axial velocity field are much more important in the production of turbulence than any feature of the secondary flowfield. Comparing Figs. 8b and 11a, we see that the mean axial velocity distortion is stronger in the common-flow-up pair than in the co-rotating pair.

The effects of varying the initial spacing of the delta wings on the co-rotating pairs at the $X = 188$-cm plane are shown in Fig. 12. For a spacing of 2 generator heights, the vortices merge quickly into a single vortex as shown in Fig. 11. For a spacing of 3 generator heights, the vortices interact strongly but do not pair in the available test section length. For spacing of 5 generator heights, the vortices' positions are only slightly modified by the presence of the other vortex.

In order to study the development of co-rotating vortices in a stable configuration and to measure their decay rate in the absence of the merging process, a regular array was constructed with a spacing of 3 generator heights. The streamwise development of the vorticity contours and of the outer axial velocity contour is shown in Fig. 13. The vortices move laterally across the tunnel at a rate approximately 1.5 times larger than an isolated vortex, due to the combined effects of all of the image vortices. The pair at the left end interact strongly, but vortices in the middle of the array appear unaffected by the ends. It should be noted that the wind tunnel was 60-cm wide, so the vortices were not constrained by the end walls as might be suggested by the figure.

The rate of vorticity spreading is quite similar to the common-flow-down vortices, indicating that the vortices in the array are essentially independent. An isolated vortex has a region of negative (secondary) vorticity on the up-wash side. However, in the co-rotating array, the primary vortex is surrounded by two regions of negative vorticity. This, apparently, has little effect on the diffusion of vorticity away from the primary vortex.

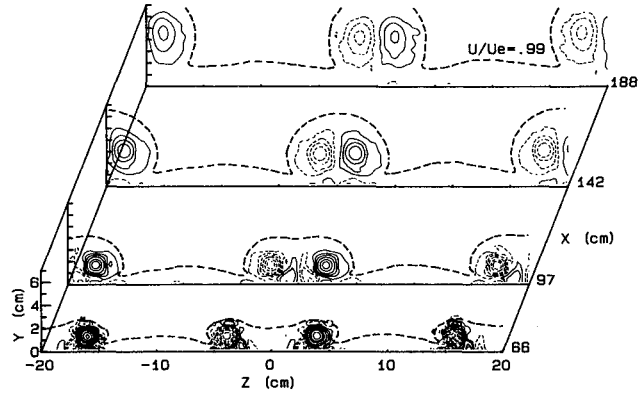

Fig. 10 Streamwise development of boundary layer with alternating vortex array with generator spacing of 10 cm; streamwise vorticity contours and 99% axial velocity contour.

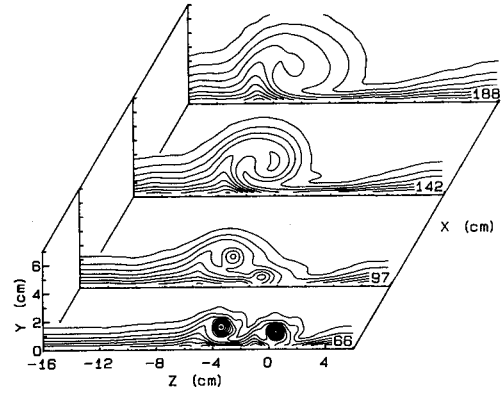

a) Contours of streamwise velocity

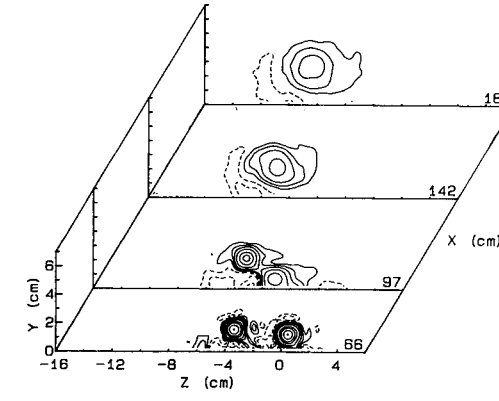

b) Contours of streamwise vorticity

Fig. 11 Co-rotating vortex pair study with 4-cm generator spacing.

IV. General Discussion and Conclusions

The results presented above indicate that the diffusion of vorticity away from a vortex is enhanced by close interaction with another vortex. The preliminary discussion also indicated that a vortex can only lose circulation by interaction with the wall, suggesting that vortices lifted far from a wall will lose circulation slowly. These statements can be made more quantitative by reference to Figs. 14–16.

Figure 14 shows the axial development of the peak vorticity for four representative cases. The vorticity decay is quite similar for the common-flow-down pair (4-cm spacing) and the co-rotating array (3-cm spacing). These vortices remain well separated from their neighbors so that secondary velocities due to one vortex are always small in the vicinity of the other vortex. The strongest vortex interaction in these cases is with the image vortex below the wall. However, this interaction is weak, since no significant flattening of the vortices is observed. The peak vorticity decays more rapidily in the two other cases shown, indicating more rapid vorticity diffusion. Both cases are common-flow-up pairs in which the two vortices of the pair interact strongly. Figures 8c and 9 show that the vorticity contours in both of these cases are strongly distorted by the secondary flow of neighboring vortex, causing more rapid spread of the vorticity.

The data of Westphal et al.[5] and the present measurements show that vorticity is diffused much more rapidly from a vortex embedded in a turbulent boundary layer than from a free turbulent vortex. Turbulence measurements for single embedded vortices presented by Westphal et al. show that the Reynolds stress field in the boundary layer is strongly distorted by the presence of the vortex. The distortions in the stress field cause enhanced diffusion of the vorticity as discussed by Perkins.[9] The present data show that a strong interaction with a neighboring vortex causes further spreading of the vorticity and a more rapid attenuation of the peak vorticity level.

Discussion of the streamwise development of the vortex circulation is more tenuous due to the uncertainties inherent in integrating the vorticity field. In calculating the circulation of a positive sign vortex, we have chosen to integrate over all of the positive vorticity in the field. This technique excludes the negative vorticity of the secondary vortex from the integration, and gives a more accurate picture of the decay of the primary vortex. In every case, the circulation of the vortex decays much more slowly than the peak vorticity. The circulation typically decreases by a factor of about 2 over the length of the test section, whereas the peak vorticity drops by a factor of 5–10. Most of the cases shown in Fig. 15 show a similar decay rate. The exception is the alternating pair array that shows a slightly slower decay rate than other cases, probably because the vortices are lifted away from the wall. A similar result would be expected for the common-flow-up vortices. However, the circulation calculation cannot be carried out beyond the 97-cm sta-

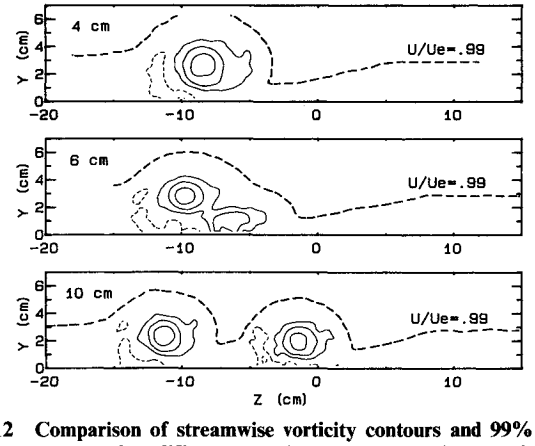

Fig. 12 Comparison of streamwise vorticity contours and 99% axial velocity contour for different spacings of co-rotating vortices at $X=188$ cm.

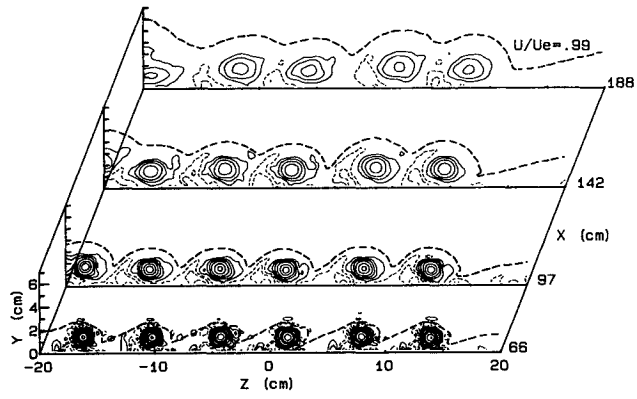

Fig. 13 Streamwise development of co-rotating vortex array with generator spacing of 6 cm; contours of streamwise vorticity and contour of 99% axial velocity contour.

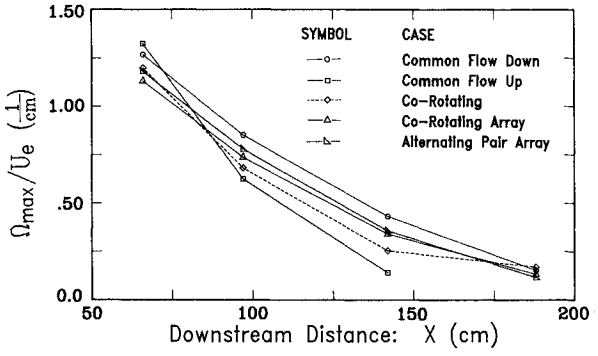

Fig. 14 Streamwise peak vorticity development for different pairs of vortices embedded in a boundary layer.

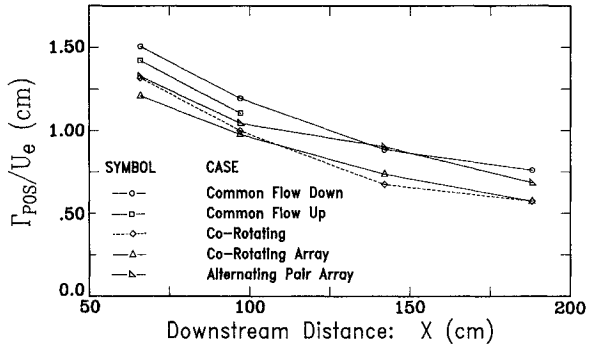

Fig. 15 Streamwise decay in vortex strength for different pairs of vortices embedded in a boundary layer.

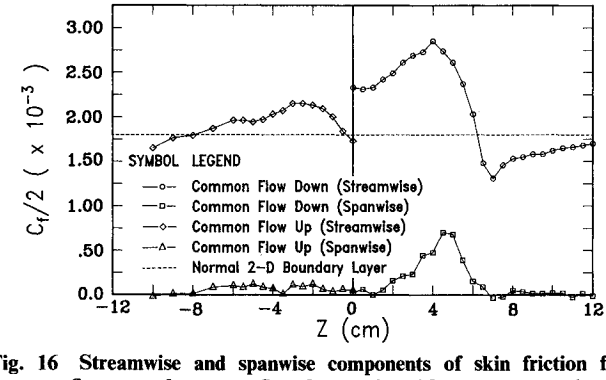

Fig. 16 Streamwise and spanwise components of skin friction for common-flow-up and common-flow-down pairs with generator spacing of 4 cm at $X=97$ cm.

tion for the common-flow-up vortices because they lift out of the measurement domain.

The primary circulation loss mechanism is the spanwise component of skin friction at the wall. Skin friction measurements presented in Fig. 16 show that the skin friction perturbation is much larger in the common-flow-down case than in the common-flow-up flow, indicating a stronger interaction with the wall. The spanwise component of the skin friction is much larger in the common-flow-down case. The spanwise skin friction for the common-flow-up case will decrease even more as the vortices continue to lift each other away from the wall.

Summarizing the above results, we have examined the interactions of several vortex pairs embedded in an otherwise two-dimensional turbulent boundary layer. Qualitatively, the vortices move about the flowfield as would be expected from potential flow theory with some allowance for the presence of induced vortices. The major mean effects of the pairs are the thickening of the boundary layer in regions where the secondary flow is away from the wall, and thinning where this flow is toward the wall.

Although close proximity of other counter-rotating vortices does not increase loss of vortex circulation, it strongly affects the spreading of the vorticity. This is seen as a more rapid drop in peak vorticity and a growth of the vortex. The direction and extent of this spreading in a vortex is controlled by the strength and proximity of other vortices. These may be actual vortices or the image vortices due to the presence of a wall. The rate at which vortex circulation decreases clearly is not proportional to the rate at which vorticity spreads through the boundary layer, but instead is governed by the proximity of the vortex to a wall.

Acknowledgments

We gratefully acknowledge the financial support of the Department of Energy Basic Energy Sciences Program (Contract DEFG0386ER-13608) and the NASA Lewis Research Center (Contract NAGz-522). Most of the experimental and data analysis techniques used were developed in close collaboration with Dr. R. V. Westphal of NASA Ames Research Center.

References

[1]Pearcy, H. H., "Shock-Induced Separation and Its Prevention by Design and Boundary Layer Control," Pt. IV, *Boundary Layer and Flow Control*, edited by G. V. Lachmann, Pergamon Press, New York, 1961, pp. 1277–1344.

[2]Spangler, J. G. and Wells, C. S., Jr., "Effects of Spiral Longitudinal Vortices on Turbulent Boundary Layer Skin Friction," NASA CR-145, Dec. 1964.

[3]Mehta, R. D., Shabaka, I. M. M. A., Shibl, A. and Bradshaw, P., "Longitudinal Vortices Imbedded in Turbulent Boundary Layers," AIAA Paper 83-0378, Jan. 1983.

[4]Westphal, R. V., Eaton, J. K. and Pauley, W. R., "Interaction Between a Vortex and a Turbulent Boundary Layer in a Streamwise Pressure Gradient," *Turbulent Shear Flows*, edited by F. Durst, B. E. Launder, F. W. Schmidt, and J. H. Whitelaw, Springer Verlag, New York, 1985, pp. 266–277.

[5]Westphal, R. V., Pauley, W. R. and Eaton, J. K., "Interaction Between a Vortex and a Turbulent Boundary Layer Part 1: Mean Flow Evolution and Turbulence Properties," NASA TM-88361, Jan. 1987.

[6]Eibeck, P. A. and Eaton, J. K. "Heat Transfer Effects of a Longitudinal Vortex Embedded in a Turbulent Boundary Layer," *Journal of Heat Transfer*, Vol. 109, No. 1, Feb. 1987, pp. 16–24.

[7]Treaster, A. L. and Yocum, A. M., "The Calibration and Application of Five-Hole Probes," *Instrument Society of America Transactions*, Vol. 18, March 1979, pp. 23–34.

[8]Higuchi, H., "A Miniature Directional Surface-Fence Gage for Three-Dimensional Turbulent Boundary Layer Measurements," AIAA Paper 83-1722, July 1983.

[9]Perkins, H. J., "The Formation of Streamwise Vorticity in Turbulent Flow," *Journal of Fluid Mechanics*, Vol. 44, Pt. 4, Oct. 1970, pp. 721–740.